Science Arts & Métiers (SAM)

is an open access repository that collects the work of Arts et Métiers ParisTech researchers and makes it freely available over the web where possible.

Identification of a 7-phase claw-pole starter-alternator for a micro-hybrid automotive application

A. Bruyère[1,2], T. Henneron[1], E. Semail[1], F. Locment[1] A. Bouscayrol[1], J.M. Dubus[2], J.C. Mipo[2]

[1]Laboratoire d'Electrotechnique
et d'Electronique de Puissance de Lille (L2EP),
Arts et Métiers ParisTech, 8, boulevard Louis XIV,
59046 Lille, FRANCE
Tel. +33 (0)3-20-62-15-61,
Fax. +33 (0)3-20-62-27-50
Email: eric.semail@lille.ensam.fr

[2]Valeo Electrical System,
2, rue André Boulle, BP 150,
94017 Créteil Cedex, FRANCE
Tel. +33 (0)1-48-98-84-37
Email: jean-claude.mipo@valeo.com

Abstract- **This paper deals with the identification of a new high power starter-alternator system, using both: a Finite Element Method (FEM) modeling and an experimental vector control. The drive is composed of a synchronous 7-phase claw-pole machine supplied with a low voltage / high current Voltage Source Inverter (VSI). This structure needs specific approaches to plan its electrical and mechanical behaviors and to identify the parameters needed for control purpose. At first, a Finite Element Method (FEM) modeling of the machine is presented. It is used for the predetermination of the electromotive forces and of the torque. Experimental results are in good accordance with numerical results. In a second part, resistive and inductive parameters of the drive are determined by an original experimental approach that takes into account each component of the drive: the battery, the VSI and the machine.**

I. INTRODUCTION

Claw-pole synchronous machines with separate excitation are commonly used to achieve the alternator function in Automotive. This is due to their low cost and their ability to work in a very large speed range. With the studied belt driven starter-alternator system [1], starting the car Internal Combustion Engine (ICE) is made with this claw-pole machine. This kind of system is used to bring the micro-hybrid Stop-Start function, without major modifications of the car powertrain. The new needed starter function adds a new constraint on the electrical machine: the ability to develop a large torque during the start. Starter-alternators already equip small cars, with a small 1.4 ICE. The major interest of this simple system concerns the limited extra cost for the final car [1], when the hybridization operation is achieved.

To take up this challenge for powerful Internal Combustion Engine (ICE) without changing the classical (12 Volts) DC-Bus voltage level [1], a new claw-pole starter-alternator with seven phases and permanent magnets between the claws has been developed [2]-[3] (Fig. 1). The obtained torque density (Nm/m^3) allows keeping the economical benefits of using a 12-Volts battery [1].

In order to carry out the starter function, a modeling of the machine is at first necessary to plan the ability of the machine to develop the torque during the short duration of the start. In section II, the predeterminations obtained by a Finite Element Method (FEM) modeling are compared with experimental results for the electromotive forces and for the torque per Ampere.

In section III, resistive and inductive parameters of the whole drive are determined. These parameters are needed for controlling the starter-alternator, in its both functioning modes: in motor mode (for the ICE start) and in alternator mode. As the voltage is low (12V), the resistive and inductive electrical parameter values of the battery and VSI are not negligible in comparison with those of the machine. At first, results obtained with classical determination approach are given and discussed. Secondly, an experimental approach based on an elementary vector control of the machine is developed to find directly the six characteristic time constants needed for controlling the seven-phase drive.

II. DETERMINATION OF EMF AND TORQUE BY FINITE ELEMENT METHOD

This kind of claw-pole structure is known to be sensitive to modeling with a numerical method as FEM [4] because of their 3D characteristics, a thin airgap (about 0.3% of the external diameter) and highly saturated magnetic materials. Moreover, the studied machine is a synchronous 7-phase claw pole machine with permanent magnets between the claws. Sixteen poles and a number of slots per pole and per phase equal to 0.25 imply a modelling of a quarter of the structure at least (Fig. 2). The aim of the modeling is not only to plan the voltage output, in generator mode, but also to determine the maximum available torque in motor mode, during the start of the car ICE. The first step in order to validate the 3D-modeling is to compare the experimental electromotive forces (emf) with the calculated ones. The second step is to obtain, for a defined repartition of the currents among the phases, the maximum possible torque.

The thin airgap leads to a mesh composed of 380000 tetrahedral elements, the air-gap being meshed with two layers

of elements. The resolution is made using the magnetostatic assumption and the scalar potential formulation, with CARMEL, a software developed at the L2EP. Fig.2 gives results of the numerical simulation, related to the magnetic flux density **B** under no load condition and a 5A current I_F supplying the excitation coil. The highest flux density values (in yellow) are obtained under the stator teeth.

Fig. 3 compares the electromotive force waveform named $e(t)$, calculated under no load condition, at a rotation speed $N = 1800$rpm and $I_F = 5$A, with an experimental measurement in the same conditions. These results validate the numerical model good accuracy, at the first order, for the determination of the voltage outputs.

Fig. 4 gives the calculated torque T as function of the rotor position θ, when the machine currents are imposed to be the same as in an experimental test (Square Wave Voltage supply), for which the torque is maximized. The maximal numerical torque value is $T_{calculated} = 62.4$ Nm, to be compared with the experimental maximum measured torque: $T_{measured} = 66.5$ Nm, that shows a difference of about 6 %.

For the determination of the inductive parameters, numerical FEM leads to too large durations of computation in the present case. It is due to the 3D characteristics of the machine and its thin air-gap (which implies a high number of 380000 elements). Moreover, the magnetic materials being highly saturated for this application, the simulation has to take into account the non-linear characteristics of the materials. In Fig. 5, the magnetic flux density is represented for a 2D slice of the whole structure (rotor and stator); z-coordinate of the slice is at the middle of the structure. This figure points out the magnetic saturation areas under no load conditions, with $i_F = 5$ A. These saturated areas evolve with the rotor position and the currents (excitation coil current i_F, and stator windings currents). They are at the origin of variable magnetic air-gap effects. As consequence, the inductances depend on the rotor position and on the currents. Finite Element modeling to calculate the inductive parameters for every rotor position, and for every supplying situation, would lead to huge computation and analysis times.

As consequence, experimental methods have been developed for the determination of the machine inductive parameters.
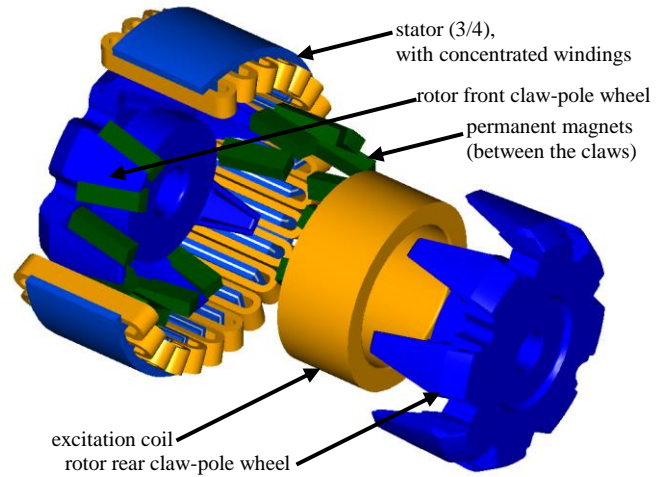

Fig.1. Exploded view of the multiphase claw pole starter-alternator
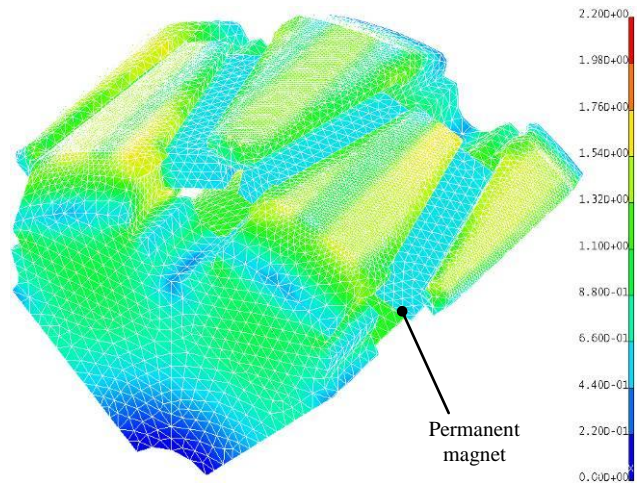

Fig. 2. Rotor magnetic flux density **B** under no-load condition with i_F=5A

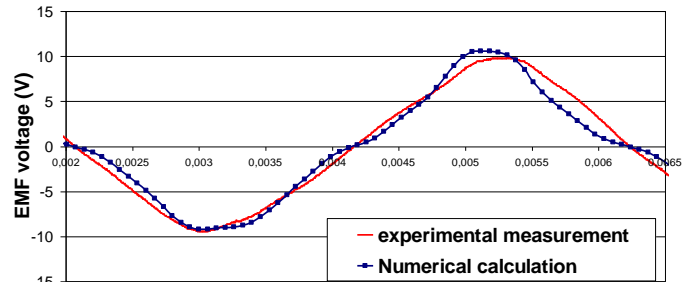Fig. 3. Electromotive force under no load condition; N=1800rpm, $I_F = 5$A and comparison with an experimental measurement
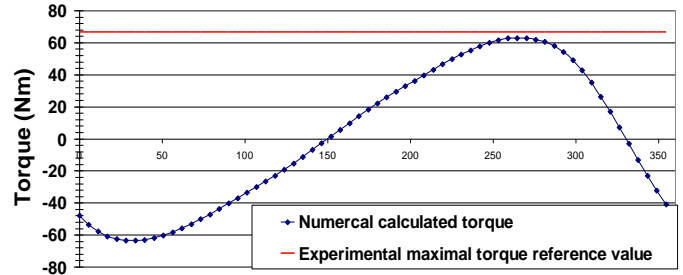

Fig. 4. Calculated torque as function of the position θ and comparison with an experimental maximal torque reference value
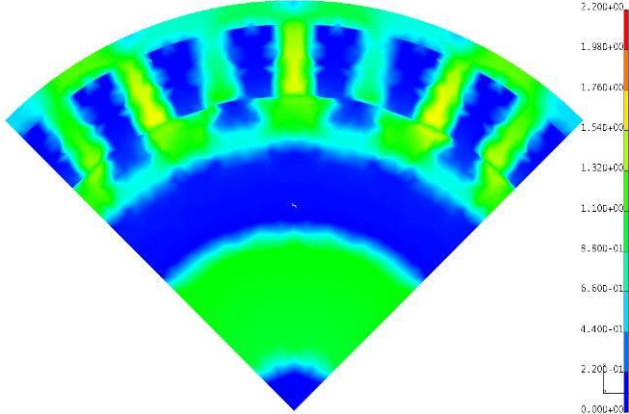
2

Fig. 5. Magnetic flux density repartition at the middle of the machine under no load condition and i_F=5A

III. INDUCTIVE AND RESISTIVE PARAMETERS IDENTIFICATION BY EXPERIMENTAL VECTOR CONTROL

In order to control the drive during transient operations, such as starts, the electrical time constants are relevant parameters since they imply the choice of the carrier frequency of the Pulse Width Modulation (PWM) for the Voltage Source Inverter (VSI). For a wye-connected three-phase machine with reluctance effects, only two time constants are sufficient to characterize the drive. As the resistance is the same in the two axis, the various values of the time constants are directly associated with those of the cyclic inductances. In comparison with conventional methods [5], more recent methods have been presented using current controls, either in the stator frame [6], or in the dq-reference frame [7]-[9]: determination of the cyclic inductances L_d and L_q can be thus obtained either indirectly or directly.

For a 7-phase machine, three different dq-reference frames, or "subspaces S1, S2 and S3", can be determined. Consequently, six time constants can be then evaluated, depending on the importance of the reluctance effects. These time constants are needed for the control.

Two methods, each one based on current control, are presented and compared in the next paragraphs. The experimental set-up is described with Appendix A2. It shows the starter-alternator directly mechanically connected to a brushless machine, used to simulate the ICE behavior. The seven-leg VSI is supplied by an electronic programmable source. A programmable electronic load is used in parallel with the voltage source in order to simulate the on-board electrical network energy consumptions. The whole system is managed using a modular dSPACE DS1006 real time control board.

A. Determination of resistance and inductance in the stator frame

The first approach is based on a simplified model. Starting from the inductances definition (1):

$$[Flux] = [L_{SS}] [I_s] \tag{1}$$

with [Flux] the seven-dimensional vector of flux linked by the seven stator phases, $[I_s]$ the associated current vector and $[L_{SS}]$ the 7X7 stator inductance matrix.

Several assumptions are made. At first, the magnetic characteristic of the materials is considered to be linear. Secondly, whereas for a seven-phase machine the $[L_{SS}]$ stator inductance matrix contains 49 values, only 7 different values, one self inductance and six mutual inductances, are considered taking into account standard assumptions of regularity, symmetry and circularity properties for this matrix. These seven inductances lead to six cyclic inductances and one homopolar inductance (or zero-sequence inductance). This last one is omitted since a wye-coupling of the machine implies that the homopolar inductance has no impact on the control.

The procedure of measurement is the following for different values of the rotor position, which is imposed and kept constant by a motion controller:

- a magnetic state is imposed by a choice of a value for the excitation current i_F;
- sinusoidal current at chosen frequency is imposed in phase n°1 by using a VSI with a control of the currents;
- voltage is measured across each phase successively;
- measured voltage is integrated. Flux and corresponding inductance are then deduced using (1).

The following measurements are made for several fixed positions. Then, Table 1 gives average values of inductances. Considering average values is in accordance with the circularity assumption used for this first method.

Practically, it has been chosen a 120 Hz frequency with a 17 A RMS sinusoidal current, around a constant 18 A current. Table I gives the average values (in µH) versus θ for two values of excitation currents.

TABLE I
INDUCTANCES VALUES (µH) IN THE STATOR FRAME

	$<L_{11}>$	$<L_{12}>$	$<L_{13}>$	$<L_{14}>$	$<L_{15}>$	$<L_{16}>$	$<L_{17}>$
i_F=0A	45	-3	-7	-3	-3	-7	-3
i_F=5A	39	-3	-6.5	-3	-3	-6.5	-3

With standard assumptions of symmetry and circularity for the $[L_{SS}(\theta)]$ stator inductance matrix, the cyclic inductances in the three d-q reference frames of the seven-phase machine are obtained by (2). In (2), L_0 is the zero-sequence inductance. The six other terms are considered by pairs, in two dimensional subspaces S1, S2 and S3 defined with the generalized Concordia transformation (denoted with the matrix [C] in (2), cf. Appendix A1). Table 2 gives the inductive parameters once the generalized Concordia transformation has been achieved. Considering separately these three subspaces, there is no difference between the inductances along the d- and q-axes. This is due to the circularity assumption of the inductance matrix (variable airgap effects are not taken into account for this first method). Table II gives average cyclic inductance values versus θ.

$$\begin{bmatrix} <L_0> & 0 & 0 & 0 & 0 & 0 & 0 \\ 0 & <L_{S1-d}> & 0 & 0 & 0 & 0 & 0 \\ 0 & 0 & <L_{S1-q}> & 0 & 0 & 0 & 0 \\ 0 & 0 & 0 & <L_{S2-d}> & 0 & 0 & 0 \\ 0 & 0 & 0 & 0 & <L_{S2-q}> & 0 & 0 \\ 0 & 0 & 0 & 0 & 0 & <L_{S3-d}> & 0 \\ 0 & 0 & 0 & 0 & 0 & 0 & <L_{S3-q}> \end{bmatrix} \quad (2)$$

$$= [C][<\boldsymbol{L_{SS}}(\theta)>][C^{-1}]$$

TABLE II
CYCLIC INDUCTANCE VALUES (μH)

I_F	$<L_0>$	$<L_{S1d}>$	$<L_{S1q}>$	$<L_{S2d}>$	$<L_{S2q}>$	$<L_{S3d}>$	$<L_{S3q}>$
0A	19	50	50	55	55	43	43
5A	14	44	44	48	48	38	38

Finally, with the knowledge of these cyclic inductances it is easy to determine the time constants, dividing the inductance by the resistance. However, using the resistance value to calculate the time constants values introduces a new uncertainty as it is detailed below.

A first approximation of the phase resistances value (R_S), using the stator windings geometrical characteristics, gives R_S = 7.6 mΩ. Measurement with a digital RLC meter bridge using a low current level (0.5 A) gives a confirmation for this winding resistance value: 8 mΩ at low frequency. However, these values concern only the machine windings. Such low resistance value implies the necessity to take into account all the parasitic resistances usually neglected: resistance of the VSI MOS transistors and resistance at the electrical connections. This uncertainty will be confirmed by the final results of this paper, using the second approach, for which the total resistance value is about 21,7 mΩ.

If this first method is theoretically easy to understand and to use, it must be also noticed that the values of inductances are weak (a few μH, especially the mutual terms of $[L_{SS}]$). So, the induced voltages are only a few Volts. Consequently, parasitic voltage drops induce uncertainties on the measurements. Moreover, the use of Concordia [C] transformation matrix implies that each determined cyclic inductance is obtained by the sum of six ones: as consequence there is an accumulation of errors on the measurements with this method.

If it will be observed in the following paragraph that the results are acceptable for average values, it must be pointed out that with this approach it is not possible to take into account the effect of all the stator currents on the values of the inductances. Fundamentally the method is based on an assumption of magnetic linearity. Basically it is thus not possible to impose to the machine a magnetic state representative of real working conditions of the drive. Nevertheless, obtained values allow a first estimation of inductive parameters and time constants. With the next approach it is possible to determine directly the cyclic inductances in conditions closed to the working ones.

B. Direct determination of time constants in dq-frames

In the studied case, since the values of resistances and inductances are very low, it is then preferable to consider a direct method of identification that takes into account implicitly the complete drive and gives directly the time constants [10]. The experimental method is based on an elementary vector control for a seven-phase machine. The control is a generalization of classical vector control in dq-reference frame developed for three-phase machines. In this case, two L_d and L_q parameters are obtained for a machine with reluctance effect (leading to 2 time constant values, on d- and q-axes). For a 7-phase machine, three different dq-reference frames, or "subspaces S1, S2 and S3", can be determined. Consequently, six time constants can be then evaluated. The principle of the control is given Fig. 6. In each subspace, there is a control of the dq-currents. The currents controllers are Proportional Integral controllers with compensation of the electromotive force. Constant current references are used except in the channel where the cyclic inductance must be identified. In this channel a simple Proportional controller is used with a square reference added to the constant reference. The PI controllers in the different channels allow ensuring a decoupling with the identified channel. The error and the closed loop time constant relative to the response to the square reference allow obtaining resistance and cyclic inductance.

Fig. 7, gives experimental results of the time constant measurements. These parameters depend on the excitation current. For one of the 3 dq-reference frames, the S1-subspace, two different values of time constants, on d- and q- axes, can be clearly identified: the difference can be explained by a variable reluctance effect in the machine. For the two others dq-reference frames, only one inductive parameter appears. These results are compared in table III and table IV with those obtained in table II for two values of I_F.

For S2 and S3 subspaces the error is satisfying (max 26 %). For S1 subspace, it appears a difference between L_d and L_q values. Indeed, the variable reluctance effect was not taken into account by the previous method because only average inductances values versus θ angle were considered. The new approach confirms that a reluctance effect is quite noticeable for the S1 subspace. If the average value $<L_{S1d}>$ obtained by the first method is compared to the average value $(L_{S1-d}+ L_{S1-q})/2$ obtained by the last approach, the relative errors are 12% for I_F=0A and 27% for I_F=0A. The results are coherent.

Fig. 6. Scheme of the vector control used for the seven-phase machine

TABLE III
COMPARISON OF AVERAGE CYCLIC INDUCTANCES FOR I_F=0A (μH)

	$<L_{S1d}>$	$<L_{S1q}>$	$<L_{S2d}>$	$<L_{S2q}>$	$<L_{S3d}>$	$<L_{S3q}>$
First method	50	50	55	55	43	43
Second method	34	54	56	54	32	36
Relative error	32	8	2	2	26	16

TABLE IV
COMPARISON OF AVERAGE CYCLIC INDUCTANCES FOR I_F=5A (μH)

	$<L_{S1d}>$	$<L_{S1q}>$	$<L_{S2d}>$	$<L_{S2q}>$	$<L_{S3d}>$	$<L_{S3q}>$
First method	44	44	48	48	38	38
Second method	19	45	46	43	28	31
Relative error (%)	57	2	4	10	26	18
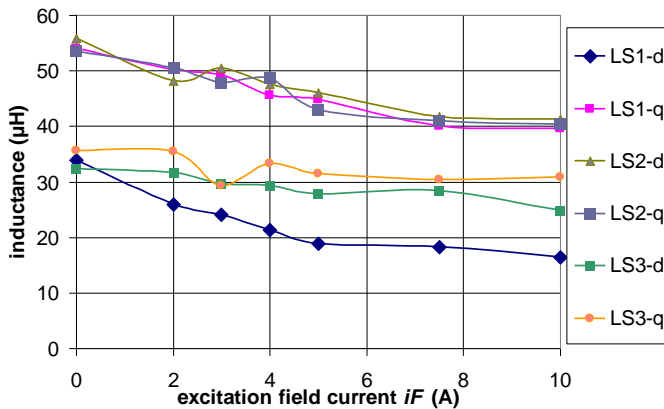
Fig. 7. Experimental inductances on d- and q- axis in the 3 subspaces as a function of the excitation current

IV. CONCLUSION

A mixed approach has been presented for the identification of a seven-phase starter-generator. The FEM modeling allows planning the main output values of the machine, as electromotive force and torque. This result is particularly interesting for the design step. A comparison with experimental results shows a good accuracy of the numerical model for the determination of these values. For parameters which are more characteristic of the whole drive such as time constants, it has been shown that the determination of inductances in the stator frame lead to uncertainties in the case of a very low voltage saturated machine. An experimental approach using a vector control has been consequently proposed in order to obtain directly the required time constants for the design of the drive.

V. REFERENCES

[1] D. Richard, Y. Dubel, "Valeo StARS Technology: A competitive Solution for Hybridization", Power Conversion Conference, PCC'07 Nagoya, Japan, pp. 1601-1605, April 2007, ISBN: 1-4244-0844-X.

[2] J. M. Dubus, A. De Vries, D. Even and J. C. Mipo: "Polyphase stator of a rotating electrical machine with claw-pole rotor and alternator or alternator starter comprising same", French Patent WO 2007/031679 A2, March 2007.

[3] F. Locment, A. Bruyere, E. Semail, X. Kestelyn, A. Bouscayrol and J. M. Dubus, "Comparison of 3-, 5- and 7-leg Voltage Source Inverters for low voltage applications", IEEE International Electric Machines and Drives Conference, IEMDC 2007, Antalya, Turkey, pp. 1234-1239, May 2007, ISBN: 1-4244-0743-5.

[4] S. Schulte, C. Kaehler, C. Schlensok and G. Henneberger, "Combined anlytical and numerical computation approach for design and optimisation of six-phase claw-pole alternators", S*cience, Measurement and Technology, IEE Proceedings* – Vol. 151, Issue 6, Nov. 2004, pp. 96 – 498.

[5] "Guide: Test Procedures for Synchronous Machines Part I Acceptance and Performance Testing Part II Test Procedures and Parameter Determination for Dynamic Analysis", IEEE Std115-1995

[6] K. M. Rahman, S. Hiti, "Identification of machine parameters of a synchronous motor", *IEEE Transactions on Industry Applications*, Vol. 41, Issue: 2, pp. 557- 565, ISSN: 0093-9994, March-April 2005

[7] B Nahid Mobarakeh, B., F. Meibody-Tabar, F., F.M Sargos, "On-line identification of PMSM electrical parameters based on decoupling control", Conf. Rec. IEEE Industrial Applications, Society Annual Meeting, Chicago, IL, USA, 2001, vol. 1, pp. 266–273

[8] D.A. Khaburi, M. Shahnazari, "Parameters identification of permanent magnet synchronous machine in vector control'. Proc. 10th European Conf. Power Electronics and Applications (EPE 2003), Toulouse, France, 2–4 September 2003

[9] Liu, L. Cartes, D.A. , « Synchronisation based adaptive parameter identification for permanent magnet synchronous motors", Control Theory & Applications, IET, July 2007, Vol 1 , pp. 1015 - 1022

[10] A. Bruyere, E. Semail, F. Locment, A. Bouscayrol, J-M. Dubus, J-C. Mipo, "Identification of sensitive R-L parameters of a multiphase drive by a vector control", IEEE Power Electronics Specialists Conference (PESC08), 6-2008
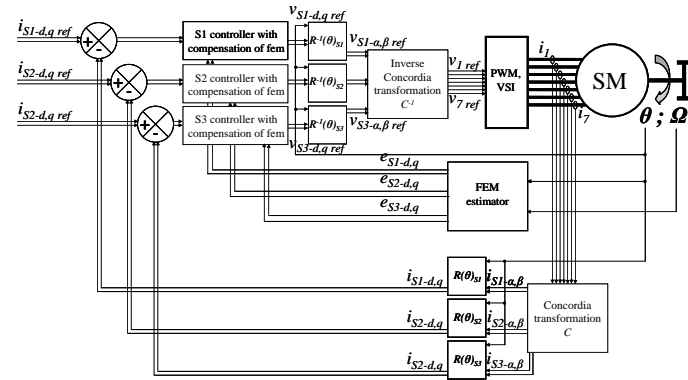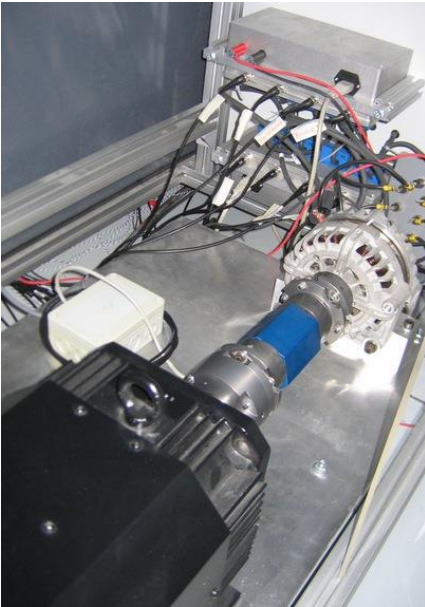
APPENDIX

A1: SEVEN-DIMENSIONAL CONCORDIA TRANSFORMATION MATRIX:

$$[C] = 1/\sqrt{7} \begin{bmatrix} \frac{1}{\sqrt{2}} & \frac{1}{\sqrt{2}}\cos\left(\frac{2\pi}{7}\right) & \frac{1}{\sqrt{2}}\cos\left(\frac{4\pi}{7}\right) & \frac{1}{\sqrt{2}}\cos\left(\frac{6\pi}{7}\right) & \frac{1}{\sqrt{2}}\cos\left(\frac{8\pi}{7}\right) & \frac{1}{\sqrt{2}}\cos\left(\frac{10\pi}{7}\right) & \frac{1}{\sqrt{2}}\cos\left(\frac{12\pi}{7}\right) \\ 0 & \sqrt{2}\sin\left(\frac{2\pi}{7}\right) & \sqrt{2}\sin\left(\frac{4\pi}{7}\right) & \sqrt{2}\sin\left(\frac{6\pi}{7}\right) & \sqrt{2}\sin\left(\frac{8\pi}{7}\right) & \sqrt{2}\sin\left(\frac{10\pi}{7}\right) & \sqrt{2}\sin\left(\frac{12\pi}{7}\right) \\ \sqrt{2} & \sqrt{2}\cos\left(\frac{4\pi}{7}\right) & \sqrt{2}\cos\left(\frac{8\pi}{7}\right) & \sqrt{2}\cos\left(\frac{12\pi}{7}\right) & \sqrt{2}\cos\left(\frac{16\pi}{7}\right) & \sqrt{2}\cos\left(\frac{20\pi}{7}\right) & \sqrt{2}\cos\left(\frac{24\pi}{7}\right) \\ 0 & \sqrt{2}\sin\left(\frac{4\pi}{7}\right) & \sqrt{2}\sin\left(\frac{8\pi}{7}\right) & \sqrt{2}\sin\left(\frac{12\pi}{7}\right) & \sqrt{2}\sin\left(\frac{16\pi}{7}\right) & \sqrt{2}\sin\left(\frac{20\pi}{7}\right) & \sqrt{2}\sin\left(\frac{24\pi}{7}\right) \\ \sqrt{2} & \sqrt{2}\cos\left(\frac{6\pi}{7}\right) & \sqrt{2}\cos\left(\frac{12\pi}{7}\right) & \sqrt{2}\cos\left(\frac{18\pi}{7}\right) & \sqrt{2}\cos\left(\frac{24\pi}{7}\right) & \sqrt{2}\cos\left(\frac{30\pi}{7}\right) & \sqrt{2}\cos\left(\frac{36\pi}{7}\right) \\ 0 & \sqrt{2}\sin\left(\frac{6\pi}{7}\right) & \sqrt{2}\sin\left(\frac{12\pi}{7}\right) & \sqrt{2}\sin\left(\frac{18\pi}{7}\right) & \sqrt{2}\sin\left(\frac{24\pi}{7}\right) & \sqrt{2}\sin\left(\frac{30\pi}{7}\right) & \sqrt{2}\sin\left(\frac{36\pi}{7}\right) \end{bmatrix}$$

A2: EXPERIMENTAL SET-UP DESCRIPTION:

(a)　　　　　　　　　　　　　　(b)　　　　　　　　　　　　　　(c)

(a): Seven-phase starter-alternator (rear of the picture) mechanically connected to a brushless synchronous machine (front of the picture)
(b): Seven-leg Voltage Source Inverter
(c): Programmable Electrical source and load